Mugla Journal of Science and Technology, Vol 3, No 2, 2017, Pages 155-159

Mugla Journal of Science and Technology

A NOVEL MULTI-BAND CHIP ANTENNA DESIGN for 2.45 GHz and 5 GHz WLAN BANDS

Bahadır S. YILDIRIM[1]

[1]Department of Electrical and Electronics Engineering, Muğla Sıtkı Koçman University, 48000, Muğla, Türkiye
bahadir.yildirim@mu.edu.tr

Received: 19.10.2017, Accepted: 19.11.2017
*Corresponding author doi: 10.22531/muglajsci.345093

Abstract

In this paper, a planar antenna operating at 2.45-GHz WLAN band, and a chip antenna operating at 2.45/5-GHz WLAN bands are presented. The chip antenna is evolved from the 2.45-GHz planar WLAN antenna. The chip antenna is, in fact, a planar shorted and folded dipole sandwiched by two FR4 layers above the circuit board. Dielectric layers above and below the radiating element form the chip-like package. The chip antenna has a small footprint of 18mm by 17mm. It has one RF signal lead and two RF ground leads for easy placement and soldering on the circuit board. 3D electromagnetic simulations have been used extensively for the design. The chip antenna exhibits good impedance and gain behavior.
Keywords: Electromagnetic analysis, chip antenna, multiple band antenna, wireless LAN, FDTD

2.45 GHz ve 5 GHz WLAN BANTLARINDA ÇALIŞAN YENİ ÇOK-BANTLI BİR YONGA ANTEN TASARIMI

Öz

Bu makalede, 2.45-GHz WLAN bandında çalışan düzlem bir anten, ve 2.45/5-GHz WLAN bantlarında çalışan bir yonga anten sunulmaktadır. Yonga anten, 2.45-GHz bandında çalışan düzlem WLAN antenden evrimleşmiştir. Yonga anten, aslında, devre kartı üzerinde bulunan iki FR4 dielektrik tabaka arasına sıkıştırılmış, kısa devre edilmiş ve katlanmış bir dipol antendir. Işıma yapan elemanın üzerinde ve altında bulunan dielektrik tabakalar yongaya benzer bir paket oluştururlar. Yonga antenin ayak izi 18mm'ye 17mm'dir. Yonga antenin devre kartı üzerinde kolaylıkla yerleştirilebilmesi ve lehimlenebilmesi için bir işaret ve iki de toprak ucu vardır. Tasarımda 3-boyutlu elektromanyetik simülasyonlar yoğun olarak kullanılmıştır. Yonga anten iyi bir empedans ve kazanç davranışı sergiler.
Anahtar Kelimeler: Elektomanyetik analiz, yonga anten, çok bantlı anten, telsiz LAN, FDTD

1. Introduction

Development of a 2.45/5-GHz multi-band WLAN chip antenna from a 2.45-GHz single-band planar WLAN antenna is presented in this paper. The single-band planar WLAN antenna is a shorted and folded, U-shaped half-wavelength dipole operating at 2.45 GHz. Dipole and patch-type antennas with shorting walls or shorting pins have been reported in the literature. Examples are the bowtie-shaped shorted patch antenna operating from 2.16 GHz to 4.13 GHz [1], a 2.4/5.8-GHz WLAN planar dipole with shorting pins and comb-shaped slots [2], a two-element PIFA array with shorting pins for 900-MHz RFID tags [3], and a planar U-shaped half-wavelength dipole for 900-MHz RFID tag applications [4]. The single-band planar WLAN antenna uses the techniques of shorting and folding of the radiating element to reduce the size, and its design is presented in Section II. Design of the multi-band WLAN chip antenna which uses the single-band antenna as a reference point, is described in Section III.

Ceramic chip antennas using meander lines [5] and helical lines [6] have been reported previously. A planar chip antenna for 2.4/5.2-GHz ISM band using meandered metal strips immersed in liquid crystal polyester (LCP) has been reported in [7]. The presented chip antenna does not need LCP material and provides full coverage for the 5-GHz WLAN band. Chip antennas using meander and spiral lines have been reported for mobile handsets [8-10]. The multi-band WLAN chip antenna differs from previous work due to unique shape of its radiating element which is sandwiched by two 1-mm thick FR4 layers. And unlike the single-band 2.45-GHz chip antenna described in [11], or the ultrawideband chip antenna described in [12], the presented chip antenna offers multiband operation in a small package. A compact WCDMA/WLAN antenna with a footprint of 20mm by 22mm [13] and a compact WCDMA/UWB/WLAN antenna with a footprint of 25mm by 25mm [14] were designed previously. The presented chip antenna has even a smaller footprint of 18mm by 17mm. Analysis of the presented antennas in this paper have been carried out using extensive 3D full-wave electromagnetic simulations by FDTD and HFSS [15].

2. Single-Band WLAN Antenna

The single-band antenna operating at 2.45 GHz was designed on a 40x48x1 (mm^3) FR4-type substrate using microstrip technology. This way, the antenna and the RF circuits can be integrated easily on the same printed circuit board (PCB). FR4-type material was selected as the substrate since it's low-cost and widely available. Fig. 1 shows the geometry of the single-band antenna. Fig. 2 shows a photograph of the fabricated antenna. Loss tangent and relative dielectric constant of FR4 are 0.02 and 4.4, respectively. The antenna is actually a shorted and folded planar half-wavelength dipole. One arm (l_1) of the dipole is realized as a conductive copper strip on the substrate. It's connected to the feeding 50-Ω microstrip line. The length of this arm is about λ/4 at 2.45 GHz. The other arm (l_2) of the dipole is realized as an extension of the RF ground on the other side of the PCB. The arm that is connected to the microstrip feeding line is shorted to the RF ground using a 7-mm long copper strip and a shorting pin. In the simulation model, the shorting pin was implemented as a copper cylinder whose diameter is 1.2 mm. Copper metallizations on the PCB have a thickness of 0.05 mm in the simulation model. The physical antenna is fed by an edge-mount SMA connector.

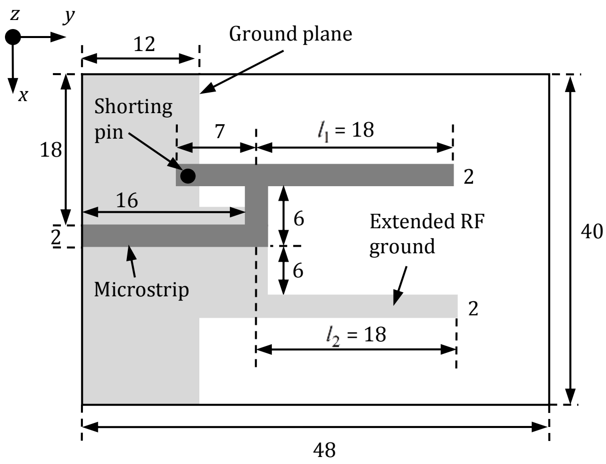

Fig. 1. Top view of the antenna geometry. All dimensions are in millimeters.

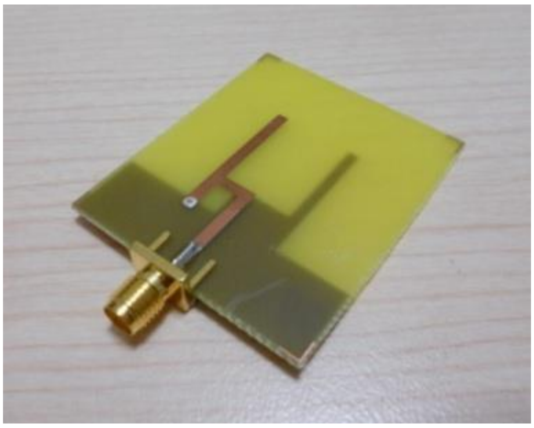

Fig. 2. Photograph of the WLAN antenna operating at 2.45 GHz.

Antenna S_{11} measurements were performed using an HP8753 20-GHz network analyzer. The antenna was connected to HP8753 using a semi-rigid coaxial cable loaded with quarter-wave long (at 2.45 GHz) RF choke sections to obtain accurate S_{11} measurements. These sections stop RF currents propagating on the exterior of the measurement cable and reduce measurement error. Fig. 3 shows measured and HFSS simulated S_{11} magnitude in decibels with and without the SMA connector up to 6 GHz. As can be seen from Fig. 3, simulated S_{11} curves are very close, with and without the SMA connector. Measurement and simulations are in excellent agreement.

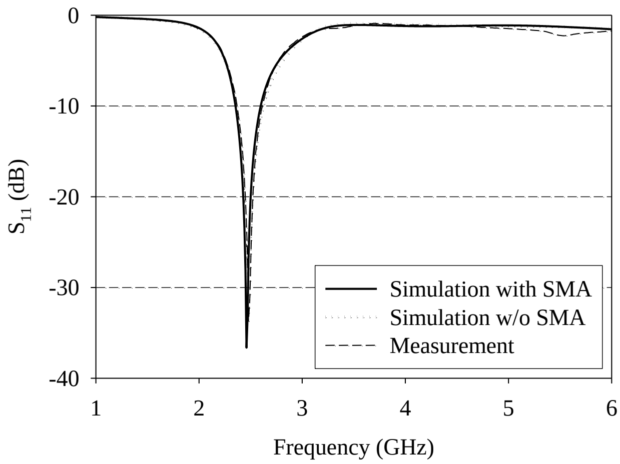

Fig. 3. S_{11} magnitude in decibels for the 2.45-GHz single-band WLAN antenna with and without the SMA connector.

Radiation patterns of the single-band antenna were measured at the Scientific and Technological Research Council of Turkey (TÜBİTAK) Antenna Test and Research Center. Probe antenna used in measurements was a wideband and double-ridged horn. The probe and the test antennas were separated by about 2.5 meters. Simulated and measured radiation patterns of the planar 2.45-GHz antenna are shown in Fig. 4 in *xy*- and *yz*-planes. Coordinate system for the planes are shown in Fig. 1. Simulations were carried out by HFSS and a FDTD (finite-difference time-domain) method. Perfectly matched layer (PML) absorbing boundaries with eight layers were implemented and a steady-state near-field to far-field transformation at 2.45 GHz were performed for FDTD radiation pattern simulations. HFSS simulation space was also terminated by an 8-layer PML boundary. The patterns were normalized to their maximum. Fig. 4 shows that the agreement between HFSS and FDTD simulations, and measurements is very good. Measurement points from about 220° to 320° were not available due to limited movement range of the positioner in the anechoic chamber. Gain of the antenna is measured about 1.4 dBi at 2.45 GHz. Distribution of the surface current at 2.45 GHz is shown in Fig. 5.

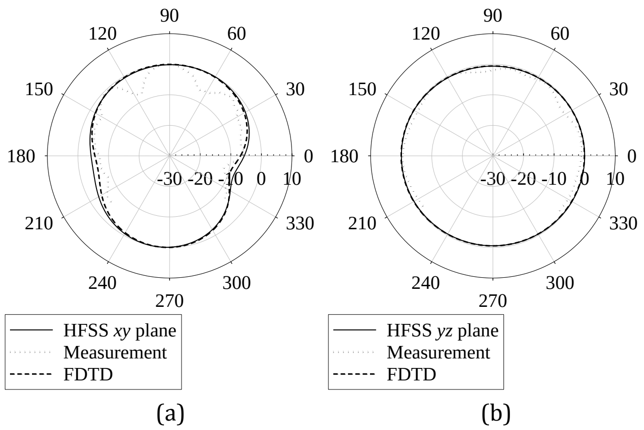

Fig. 4. Patterns of radiation of the single-band WLAN antenna at 2.45 GHz in (a) *xy*-plane, and (b) *yz*-plane.

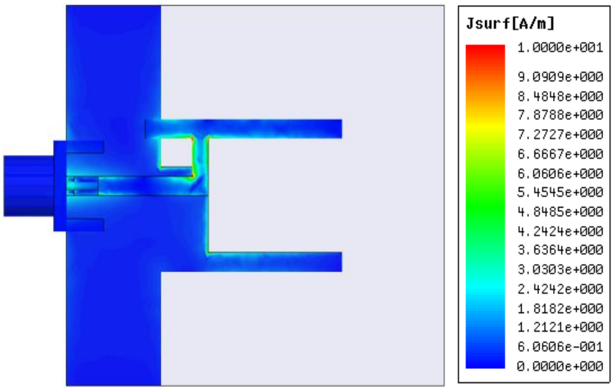

Fig. 5. Simulated surface current density at 2.45 GHz.

3. Multi-Band WLAN Chip Antenna

The chip antenna geometry is shown in Figs. 6-7 and how it's evolved from the single-band planar WLAN antenna can be seen by comparing Figs. 1 and 6-7. Basically, the radiating element of the single-band planar WLAN antenna was raised above the circuit board by 1 mm, and sandwiched between two 1-mm thick FR4 layers. Dielectric layers above and below the radiating element form the chip-like package. Three leads are extended from the radiating element. The center lead has dimensions of 2x4 (mm^2) and connected to the feeding 50-Ω microstrip transmission line whose width is also 2 mm. The RF ground lead whose dimensions are 6x4 (mm^2) makes connection between the circuit board's RF ground and the chip's internal RF ground through three shorting pins. The other RF ground lead whose dimensions are 4x4 (mm^2) shorts the conductive strips within the chip package to ground through two shorting pins. This configuration allows the chip antenna to be moved and soldered on the PCB just like any other component, though effect of the RF ground has to be investigated for proper placement prior to soldering on a specific PCB. The shorting pins have been implemented as copper cylinders whose diameter is 1.2 mm for the simulations. Thickness of the copper metallization for the radiating element and the microstrip line are taken as 0.035 mm for the simulation model. 5-GHz WLAN band is generated due to coupling between 6x1 (mm^2) and 6.5x1 (mm^2) strips. Since the simulations with and without the SMA connector are almost the same for the single-band antenna, SMA connector was not used in the simulation model of the chip antenna.

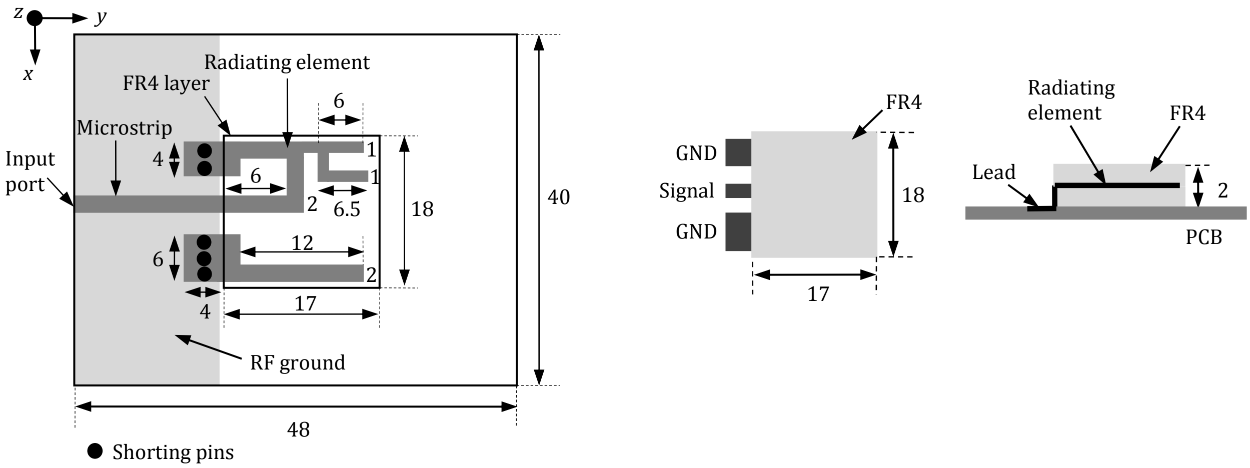

(a) (b)

Fig. 6. The chip antenna geometry, (a) radiating element, (b) top and side views. All dimensions are in millimeters.

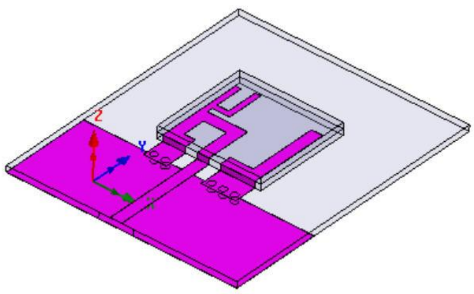

Fig. 7. 3D simulation geometry of the chip antenna.

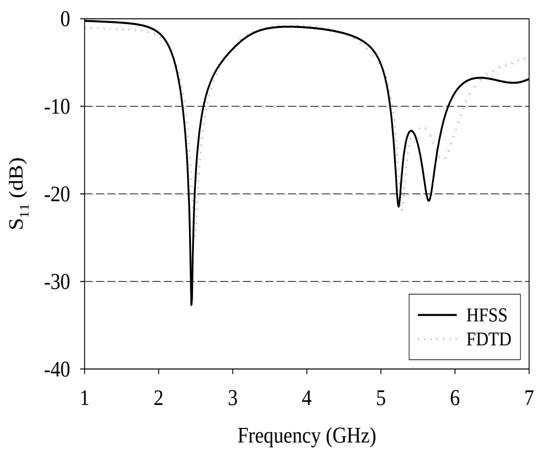

Fig. 8. The chip antenna S_{11} simulations.

S_{11} simulations of the chip antenna, performed by HFSS and FDTD method, are shown in Fig. 8. Comparison of simulations shows that both techniques are in very good agreement. Fig. 8 shows that the antenna low-band exists from about 2.3 GHz to 2.6 GHz, whereas the high-band exists from about 5.1 GHz to about 6 GHz, and includes the entire 5-GHz WLAN band.

Antenna impedance bandwidth is determined by S11 ≤ -10 dB criterion which corresponds to inside of the VSWR 2:1 circle on the Smith Chart. There is a small disagreement between FDTD and HFSS simulated S_{11} above 5.5 GHz. This may be due to discrete and uniform nature of the FDTD cells used in calculations. Radiation pattern simulations of the chip antenna are shown in Figs. 9 and 10. The pattern of radiation at 2.45 GHz, shown in Fig. 9, reveals that the antenna is omni-directional. The simulated value of peak directivity is about 1.7 dBi at 2.45 GHz whereas it is about 4 dBi at 5.8 GHz. The pattern of radiation at 5.8 GHz exhibits a more complex behavior than that of the 2.45 GHz pattern due to shorter wavelength. HFSS and FDTD simulated patterns of radiation are in excellent agreement.

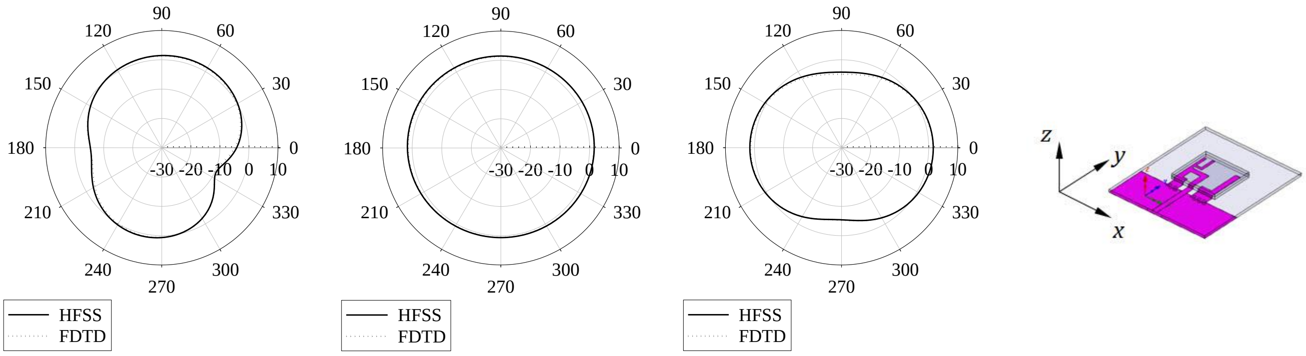

(a) (b) (c) (d)

Fig. 9. Simulated patterns of radiation (directivity) of the chip antenna at 2.45 GHz in (a) *xy*-plane, (b) *yz*-plane, (c) *xz*-plane, and (d) the coordinate system.

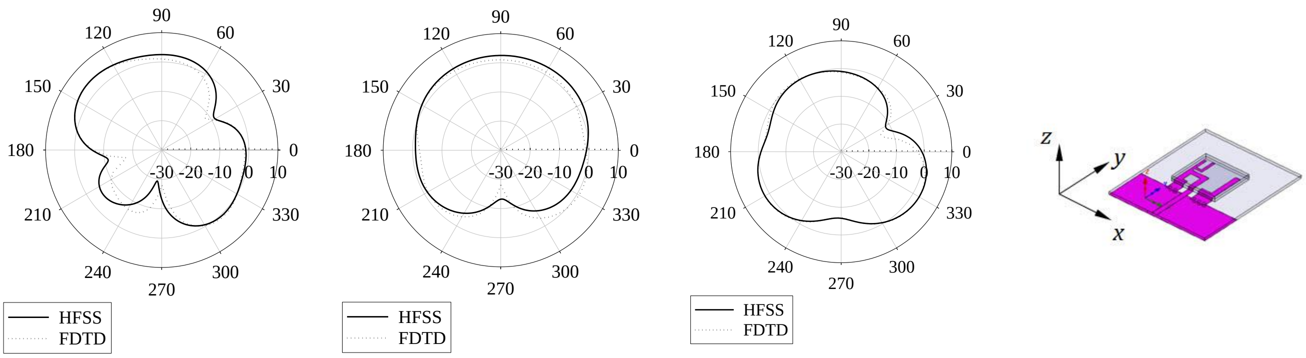

(a) (b) (c) (d)

Fig. 10. Simulated patterns of radiation (directivity) of the chip antenna at 5.8 GHz in (a) *xy*-plane, (b) *yz*-plane, (c) *xz*-plane, and (d) the coordinate system.

HFSS calculated directivity and realized gain are shown in Fig. 11. From 2.1 GHz to 2.8 GHz, directivity is about 1.7 dBi. At high-band, directivity varies from about 3.5 dBi to 4.2 dBi. Realized gain includes the mismatch loss and the loss due to FR4 material, and for these reasons, it's lower than directivity. The chip antenna exhibits good gain performance. Calculated surface currents are shown in Fig. 12. The coupling between 6x1 (mm²) and 6.5x1 (mm²) strips on the radiating element generates the 5-GHz WLAN band, and this is evident from Fig. 11(b) since the current magnitude is higher on these strips at 5.8 GHz.

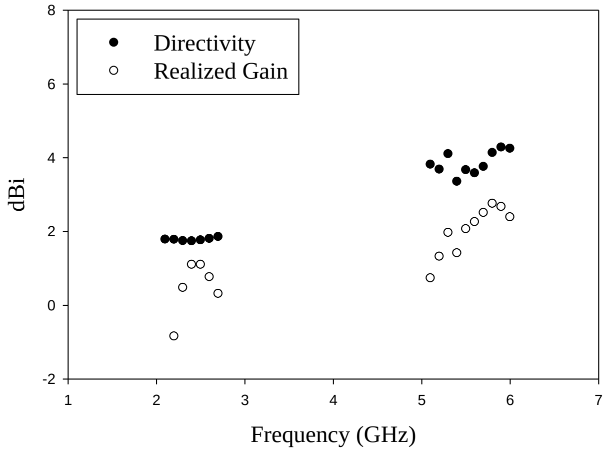

Fig. 11. Calculated directivity and realized gain of the chip antenna.

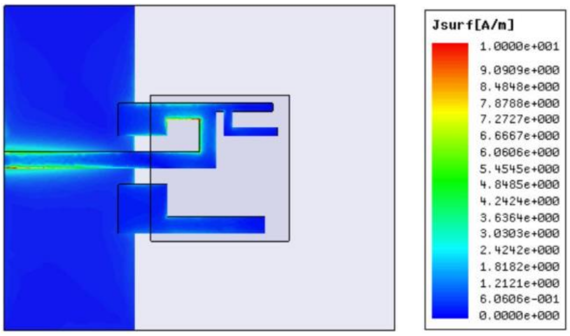

(a)

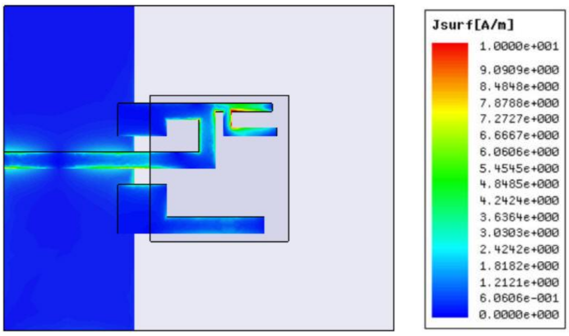

(b)

Fig. 12. Simulated surface current densities at (a) 2.45 GHz and (b) 5.8 GHz.

4. Conclusion

A planar single-band antenna for 2.45-GHz WLAN applications, and a compact, multi-band, chip-type antenna for 2.45/5-GHz WLAN applications have been presented. The chip antenna is evolved from the planar single-band WLAN antenna by placing the radiating element between two 1-mm thick FR4 layers above the PCB. It's compact in size, has a footprint of 18mm by 17mm, and has three soldering leads for easy placement on the PCB. The gain and impedance properties of the chip antenna are very good. It can be used as a multi-band WLAN antenna in mobile platforms.

5. Acknowledgment

The author thanks to Assist. Prof. Dr. Erkul Başaran and Prof. Dr. Bahattin Türetken for their help with antenna measurements.

6. References

[1] Wong H., Mak K.-M., and Luk K.-M., "Wideband shorted bowtie patch antenna with electric dipole", *IEEE Transactions on Antennas and Propagation*, Vol. 56, No. 7, pp. 2098 - 2101, July 2008.

[2] Chen J.Y., Zhang X.M., Wang H., and Sun J.Q., "A dual-band dipole with shorting pins and slots", *Proceedings of International Symposium on Signals, Systems and Electronics*, pp. 1-3, 2010.

[3] Chen H.-D. and Tsao Y.-H., "Low-profile PIFA array antennas for UHF band RFID tags mountable on metallic objects", *IEEE Transactions on Antennas and Propagation*, Vol. 58, No. 4, pp. 1087-1092, 2010.

[4] Lee S., Jung H., Choo H., and Park I., "Design of a U-shaped RFID tag antenna with an isotropic radiation characteristic", *International Workshop on Antenna Technology (iWAT)*, pp. 306-309, 2011.

[5] Choi W., Kwon S., and Lee B., "Ceramic chip antenna using meander conductor lines," *IEE Electronics Letters*, Vol. 37, pp. 933-934, July 2001.

[6] Sim S.H., Kang C.Y., Yoon S.J., Yoon Y.J., and Kim H.J., " Broadband multilayer ceramic chip antenna for handsets", *IEE Electronics Letters*, Vol. 38, pp. 205-207, Feb. 2002.

[7] Fang C.-Y., Cheng L.-S., Li J.-H., Yang C.-Fa, Lin J.-H., Liao C.-L, Chen C.-H., Lin S.-T., Cheng K.-C., Wang S.-F., Pan M.-C., Hu C.-L., and Chien Y.-C., "A planar chip antenna for 2.4/5.2GHz ISM band applications", *Antennas and Propagation Society International Symposium*, pp. 455-458, 2005.

[8] Choi H., Shin D., Kim M., and Kim H., "A design of miniaturized built-in penta band chip antenna for EGSM/GPS/DCS/USPCS/WCDMA mobile handset," *Proceedings of Asia-Pacific Microwave Conference*, 2006.

[9] Park S., Kim H., Choi H., Cho J., and Kim H., "A design of multiband chip antenna with the shorting pin for mobile handsets," *The Second European Conference on Antennas and Propagation EuCAP 2007*, pp. 1-4, 2007.

[10] Kim H., Choi H., Park S., and Kim H., "Chip antenna using three branch structures and interdigitated gap feeding" *Proceedings of Asia-Pacific Microwave Conference*, 2007.

[11] Liu H.-W., Chen T.-Y., Yang C.-F., Lin S.-T., Tasi S.-S., Chiu C.-W., and Hu C.-L., "A miniature chip antenna without empty space on PCB for 2.4GHz ISM band applications," *Antennas and Propagation Society International Symposium*, pp. 1-4, 2008.

[12] Lee J.-N., Park J.-K., and Kim J.-S., "Design of compact chip antenna for UWB applications", *IEEE International Conference on Ultra-Wideband (ICUWB)*, pp. 155-158, 2009.

[13] Yildirim B., Basaran E., and Turetken B., "Dielectric loaded compact WLAN/WCDMA antenna with shorted loop and monopole elements", *IEEE Antennas and Wireless Propagation Letters*, vol. 12, pp. 288-291, 2013.

[14] Yildirim B.S., Basaran E., and Turetken B., "Compact and Planar WCDMA/WLAN/UWB Antenna with Shorted Loop and Monopole Elements", *ACES Journal, vol. 31, pp. 288-293*, 2016.

[15] Ansoft HFSS version 11, *3D EM-Field Simulation for High Performance Electronic Design*, Pittsburgh, PA, USA: Ansoft Corporation.

Mugla Journal of Science and Technology